

Change in the surface state of the single-crystal germanium as a result of implantation with silver ions and annealing with light pulses

© T.P. Gavrilova, B.F. Farrakhov, Ya.V. Fattakhov, S.M. Khantimerov, V.I. Nuzhdin, A.M. Rogov, V.F. Valeev, D.A. Kononov, A.L. Stepanov

Zavoisky Physical-Technical Institute, FRC Kazan Scientific Center of RAS,
420111 Kazan, Russia
e-mail: tatyana.gavrilova@gmail.com

Received June 15, 2022

Revised July 12, 2022

Accepted August 12, 2022

Single-crystal *c*-Ge plates implanted with Ag⁺ ions with an energy of $E = 30$ keV, current density of the ion beam $J = 5 \mu\text{A}/\text{cm}^2$ and a dose of $D = 2.5 \cdot 10^{16}$ ion/cm² were subjected to rapid thermal annealing by single light pulses of various durations from 1 up to 9.5 s. By scanning electron microscopy and optical reflection spectroscopy measurements it was shown that after ion implantation an amorphous porous Ag:PGe layer of spongy structure, consisting of Ge nanowires, is formed on the surface of *c*-Ge substrates. It was found that the annealing with an increase in the pulse duration up to 5 s successively leads to an increase in the Ge nanowire diameters from 26 to 35 nm. With longer pulses, the porous Ag:PGe structure is destroyed and Ag evaporates from the implanted layers.

Keywords: nanoporous germanium, ion implantation, rapid thermal annealing.

DOI: 10.21883/TP.2022.12.55194.159-22

Introduction

At present, for fast and efficient modification of the structure and properties of various ion-implanted semiconductor materials the annealing technologies with light pulses with different width (τ) are widely used. These technologies, which differ by τ , include: (1) annealing by coherent laser pulses with $\tau = 1-1000$ ns; (2) annealing with gas-discharge flash lamps with $\tau = 100 \mu\text{s}-100$ ms, and (3) fast thermal annealing (FTA) carried out by halogen lamps at much higher values of $\tau = 1-100$ s [1]. The main difference between these technologies when affecting a semiconductor material is the depth of heating and the degree of modification of the surface layer. Note that in the case FTA, the greatest depth is achieved.

One of the interesting objects subjected to annealing using gas-discharge flash lamps are thin layers of nanoporous germanium (PGe) formed by ion implantation. In this paper [2] by implantation of ¹¹⁹Sn⁺ heavy ions into single-crystal *c*-Ge substrates at energy $E = 150$ keV, the current density in the ion beam $J = 0.35 \mu\text{A}/\text{cm}^2$ and doses $D = 1.4 \cdot 10^{15}-4.2 \cdot 10^{15}$ ion/cm² the layers Sn:PGe 300 nm thick were formed, consisting of open pores of a column-type structure similar to a honeycomb. These Sn:PGe layers were used to study the possibilities of annealing using gas-discharge flash lamps with $\tau = 3$ ms. According to Raman spectroscopy studies the annealed Sn:PGe layers were characterized by a crystal structure containing the GeSn alloy. In this case, it was suggested that the observed recrystallization of the implanted layer occurs due to solid-phase epitaxy. On the whole, the honeycomb structure of Sn:PGe was retained after annealing, although its partial destruction or melting was observed in local

places on the sample surface. Thus, the paper [2] demonstrates the principle possibility of changing the morphology of the Sn:PGe layer formed by ion implantation by short light pulses.

Relatively recently [3] it was shown that it is possible to create an anode of a lithium-ion battery based on Ag:PGe, formed by Ag⁺ ions implantation. It is obvious that the efficiency of anode operation during battery charging/discharging is directly determined by the PGe structure and the presence of a large pore wall surface. Therefore, it is of interest to experimentally evaluate the possibility of modifying the morphology of the implanted Ag:PGe layer by annealing with incoherent light pulses by analogy with the procedure given the work [2]. However, in contrast to annealing with short light pulses [2], in this study, for the first time, the results on FTA were obtained, i. e. annealing with a longer duration τ , on Ag:PGe structures, which, as the literature data show, were not previously considered as an object for light annealing.

1. Experiment procedure

The role of substrates for the ion implantation was played by polished plates *c*-Ge with n-type conductivity, 700 μm thick with crystal-lattice orientation (111). The implantation was realised by ions of Ag⁺ with $E = 30$ keV, $D = 2.5 \cdot 10^{16}$ ion/cm² at $J = 5 \mu\text{A}/\text{cm}^2$ by ILU-3 ion accelerator at a normal angle of the ion beam incidence to the surface *c*-Ge, the details of which are described in paper [4]. Fast thermal annealing of the implanted samples Ag:PGe was carried out with a modernized unit „Impulse-6“, in which halogen lamps located in a sealed

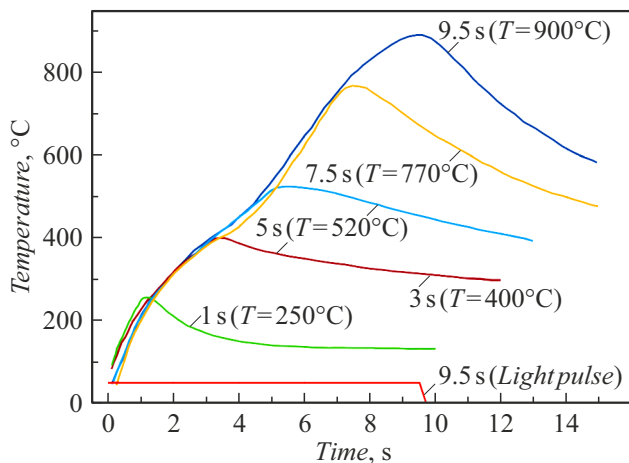


Figure 1. Diagrams of the temperature change for the implanted samples Ag:PGe as function of time at during FTA for light pulses with different τ . In parentheses the maximum values of the sample surface temperature for each τ are given. As an example, the shape of light pulse with $\tau = 9.5$ s measured by a photodiode is shown.

reaction chamber are used as heating elements. Light exposure was carried out by a single pulse with different values of $\tau = 1$ –9.5 s. The temperature was monitored using a chromel-alumel thermocouple, which was in close contact with the rear surface of the substrate, and the light pulse shape was monitored by a FD-24K photodiode. The unit was connected to a control computer, on which the experimental data on temperature and the light pulse shape were stored and displayed on the monitor screen. To reduce the inertia and the thermocouple influence on the temperature of the semiconductor, the thermocouple was made of thin wires with a diameter of $100\ \mu\text{m}$.

Fig. 1 shows diagrams of the temperature change of the implanted samples Ag:PGe from time during FTA. The maximum temperatures on the surface of the samples ($T = 250$ – 900°C), corresponding to pulses with different τ , are also shown in Fig. 1. The diagrams show inhomogeneous dynamics of sample heating. For the shortest light pulse with $\tau = 1$ s, there is an abrupt temperature rise up to $T = 250^\circ\text{C}$ and its rapid decrease after the end of the light pulse. For light pulses with greater τ there is a long-time monotonic rise and a gradual decreasing of the sample temperature. For the convenience of the experimental results description, the samples by the value of the maximum temperature achieved during the FTA: 250, 400, 520, 770 and 950°C were denoted.

The study of the surface morphology of the samples and energy-dispersive (EMF) analysis were carried out using a scanning electron microscope (SEM) Merlin (Carl Zeiss). The optical reflection spectra were measured with AvaSpec 2048 spectrometer (Avantes) at a normal angle of incidence of the probing and reflected light beam to the surface of the samples through a coupled waveguide in the spectral range from 220 to 1100 nm. Measurements of current-

voltage characteristics (CVC) of implanted and annealed layers Ag:PGe were carried out with an original unit at room temperature in the current range from -5 to 5 mA and voltages from -16 to 3.5 V when using tungsten probes. A probe from the side of the annealed surface was used as one of the contacts. The second contact on the substrate side — the sample was placed on a conductive polished aluminum plate, which served as the second contact.

2. Results and discussions

The SEM image of the Ag:PGe sample surface formed by implantation with Ag^+ ions, as well as the size distribution histogram of Ge nanowires, are shown in Fig. 2. The SEM image looks similar to the sponge-like structures seen earlier the work [4]. As can be seen from Fig. 2, under the chosen conditions of ion implantation the maximum of the diameter distribution histogram corresponds to 26 nm.

Fig. 3 shows SEM images of Ag:PGe layers after annealing by light pulses with $\tau = 1, 3$ and 5 s, which caused the samples to be heated to $T = 250, 400$ and 520°C respectively. Spongy structure is preserved on all samples. In this case, the dynamics of a monotonic increase in the diameter ($29, 31,$ and 35 nm) of Ge nanowires in annealed samples is observed simultaneously with the rise of maximum surface heating temperature.

Previously, it was supposed that the increase in the diameter of nanowires during heating of the Ag:PGe sample [4] could be due to the mechanism of Ostwald ripening [5]. This is facilitated by a decrease in the melting temperature of Ge relative to the value of the bulk material $T_{\text{Ge}} = 938.25^\circ\text{C}$ with a decrease in the dimension of its structure. For example, in the work [6] it was experimentally shown that the melting temperature of Ge nanoparticles 20 nm in size is about 600°C . Therefore, when the Ag:PGe layer is heated to a given temperature,

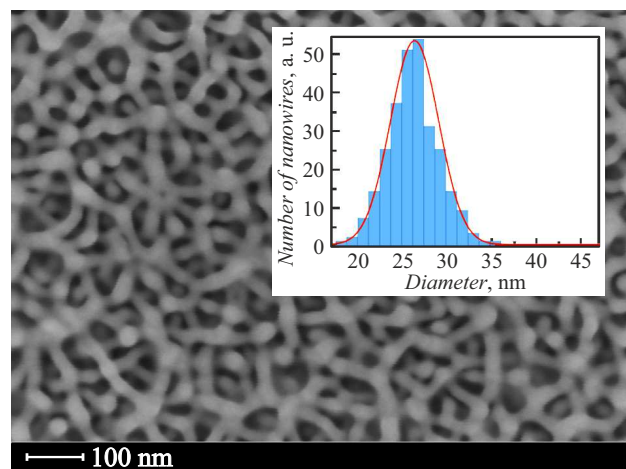


Figure 2. SEM image of *c*-Ge surface implanted with Ag^+ ions at $E = 30$ keV, $J = 5\ \mu\text{A}/\text{cm}^2$ and $D = 2.5 \cdot 10^{16}$ ion/ cm^2 . The insert shows a histogram of the Ge nanowire diameter distribution.

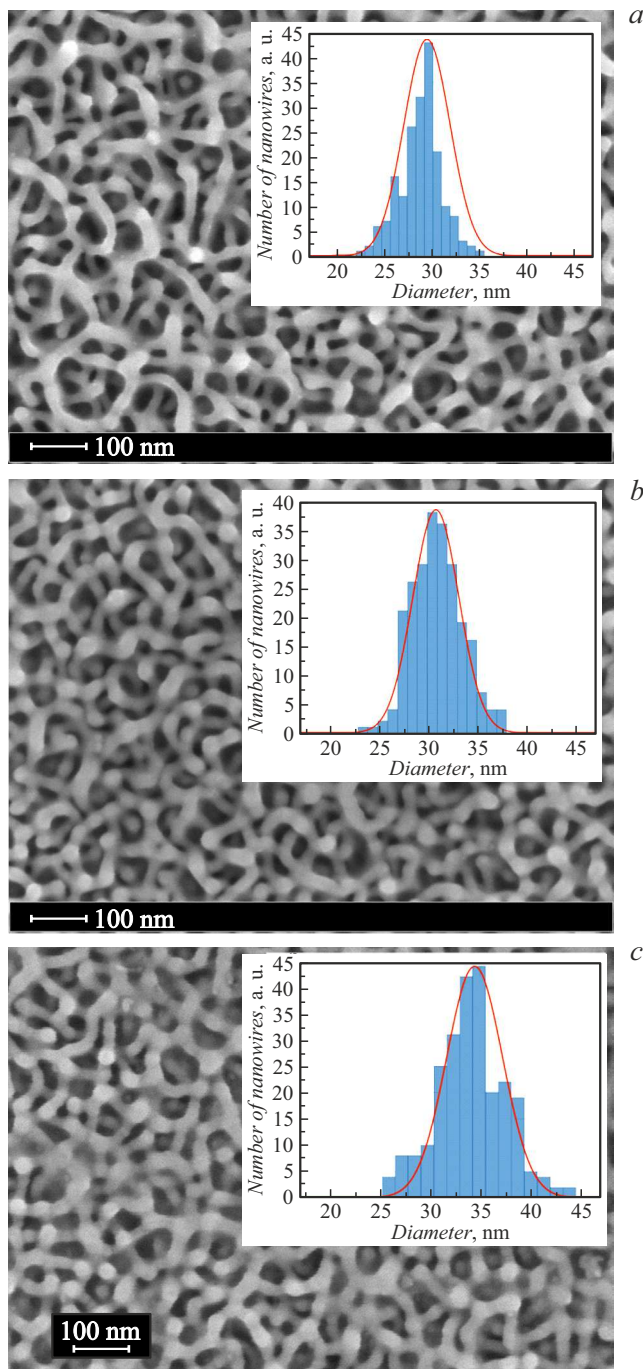


Figure 3. SEM images of surfaces of Ag:PGe samples subjected to FTA by light pulses with different τ , s: *a* — 1 ($T = 250^\circ\text{C}$); *b* — 3 ($T = 400^\circ\text{C}$) and *c* — 5 ($T = 520^\circ\text{C}$). The insets show histograms of Ge nanowire diameter distribution.

under the action of light pulse the individual thinnest nanowires melt with natural displacement of the liquid material by surface tension forces. The Ge atoms released in this case could diffuse and integrate into the structure of undestroyed PGe nanowires, increasing their diameter. In this case, the possibility of thin wires destruction due to thermal enhancement of surface diffusion, leading towards

decreasing of the surface energy of the system, cannot be excluded.

The dynamics of the diameter increasing of Ge nanowires observed in Fig. 3 with the temperature increasing of the sample during FTA qualitatively confirms the mechanism of Ostwald ripening, since with temperature increasing one should expect the melting of a larger number of nanowires, including those with larger diameters. However, as follows from Fig. 4, when using the light pulse with τ exceeding 5 s and, accordingly, sample temperature increasing above $T = 520^\circ\text{C}$ (Fig. 3), the complete melting occurs of spongy porous structure. The SEM image in Fig. 4, *a* demonstrates that after FTA at $\tau = 7.5$ s and reaching the temperature $T = 770^\circ\text{C}$, the Ag:PGe layer is absent. The sample surface consists of alternating micron-sized regions, similar to the smooth surface of *c*-Ge, surrounded by torn melted terraces. Annealing with light pulse with $\tau = 9.5$ s heats the sample to temperature $T = 900^\circ\text{C}$, comparable to the melting point T_{Ge} of the bulk material, which also leads to the appearance of melted terraces on the sample surface (Fig. 4, *b*). However, the SEM image of the same sample with a lower magnification (Fig. 4, *c*) additionally shows that, as a result of heating and melting of the porous layer the spherical formations up to $5\ \mu\text{m}$ in size are formed on the terraces, they are randomly distributed over the surface.

The EDX measurements of the unannealed Ag:PGe sample indicate in the spectra the presence of lines near 2.5 keV corresponding to Ag. After FTA with $\tau = 1, 3$ and 5 s Ag-peaks are also present in the EDX spectra. At the same time, when using light pulses with higher τ values, the presence of Ag in the annealed samples is not detected. This circumstance indicates that at high FTA temperatures in addition to the melting process the intense evaporation of alloying atoms from the surface of heated samples occurs, which leads to the loss of implanted Ag.

Fig. 5 shows the optical reflection spectra of the *c*-Ge substrate, the Ag:PGe sample formed by ion implantation, and its surface after FTA by light pulses with different τ . The spectrum of unimplanted *c*-Ge consists of several bands with maxima near 276, 564 and 820 nm, corresponding to intraband and interband electronic transitions [7]. The intensity of the 276 nm band characterizes the degree of crystallinity of the semiconductor material [8]. The *c*-Ge substrate implantation with Ag^+ ions leads to abrupt decrease in the intensity of the reflection bands with maxima at 276 and 564 nm (Fig. 5), which indicates the sample surface amorphization and the formation of porous layer Ag:PGe, as was previously studied in detail in the work [9]. The effect of reflection decreasing upon surface amorphization of Ge implanted with Ni^+ and O^+ ions was discovered in the works [10,11], respectively. The sample darkening, known in the literature as „black Ge“, occurs due to increase in Rayleigh scattering by the Ag:PGe nanoporous structure, which also leads to decrease in optical reflection [12].

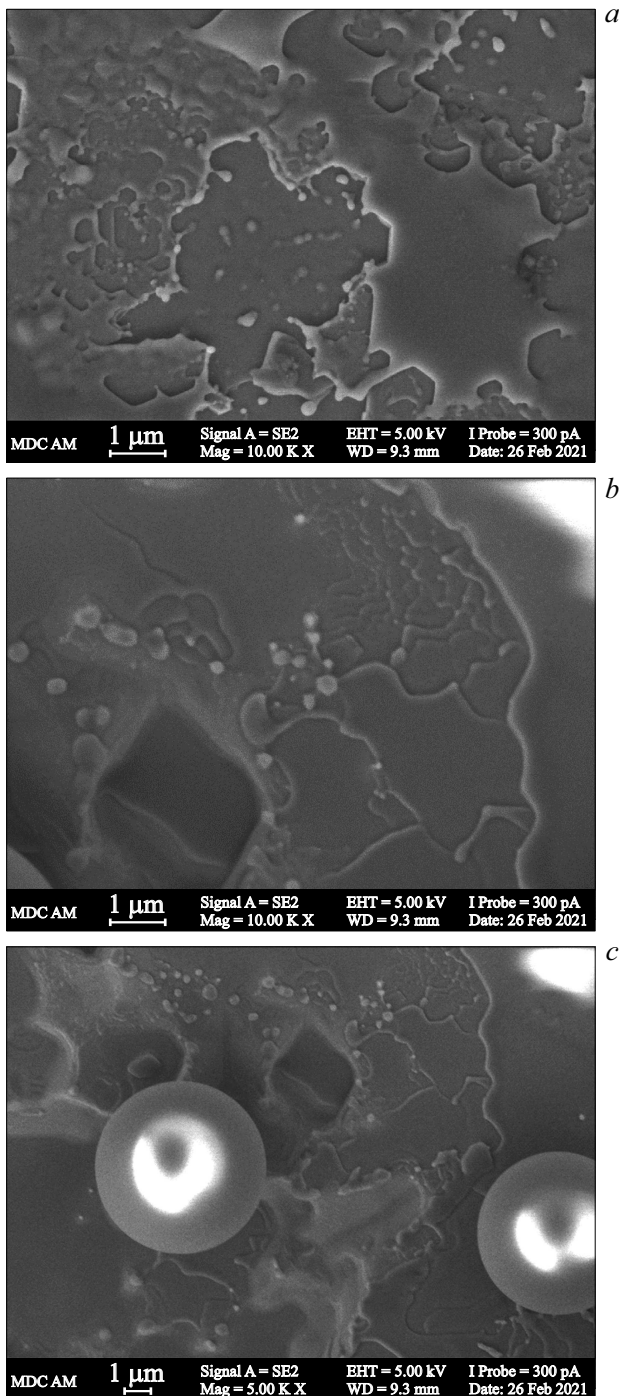


Figure 4. SEM images of surfaces of Ag:PGe samples subjected to FTA by light pulses with different τ , s: *a* — 7.5 ($T = 770^\circ\text{C}$); *b*, *c* — 9.5 ($T = 900^\circ\text{C}$). A micrograph (*c*) corresponds to a large scale SEM image (1 μm).

Fast thermal annealing ($\tau = 1$ s, $T = 250^\circ\text{C}$) of the Ag:PGe sample leads to decrease in the optical reflection intensity in the near ultraviolet region relative to the unannealed material, while in the other part of the optical range the shapes of the spectral lines practically coincide. It could be assumed that the observed decrease in reflection

occurs due to increased Rayleigh light scattering [12], since, as shown in Figs 2 and 3, *a*, the Ge nanowires diameter increased from 26 to 29 nm. However, during FTA ($\tau = 3$ s, $T = 400^\circ\text{C}$; $\tau = 5$ s, $T = 520^\circ\text{C}$) of Ag:PGe samples, in contrast to the reflection spectrum for $T = 250^\circ\text{C}$, an increase in the intensity of the band with maximum at 276 nm by approximately 10% is observed. Despite the increase in the diameter of Ge nanowires to 35 nm (Fig. 3, *c*) and the accompanying increase in Rayleigh scattering, the effect of partial crystallization of the amorphous implanted Ag PGe layer appears, leading to reflection increasing at the short-wavelength part of the spectrum. In the works [13,14] using the method of Raman spectroscopy it was also shown that amorphous layers consisting of Ge nanowires, formed by an electrochemical method, after heating them with He–Ne-laser demonstrate partial restoration of Ge crystal lattice.

During FTA ($\tau = 7.5$ s, $T = 770^\circ\text{C}$; $\tau = 9.5$ s, $T = 900^\circ\text{C}$) of Ag:PGe reflectance spectra correspond to the spectra of surfaces without Ge nanowires (Fig. 4), but containing micron-sized terrace formations. Such large formations lead to a shift of the wide spectral band of Rayleigh scattering of light from the ultraviolet to the long-wavelength region of the optical range, which significantly reduces the integral reflection over almost the entire visible range [15]. These low-intensity reflection spectra are close to the spectra of antireflection structures created on Ge surface by electrochemical methods [12]. The presence of a band with maximum at 276 nm also indicates that at these annealing temperatures the process of partial recrystallization of the implanted layer occurs.

CVC of the original substrate of *c*-Ge sample with the implanted Ag:PGe layer, as well as of the same sample subjected to FTA, are shown in Fig. 6. CVC for the substrate *c*-Ge of *n*-type demonstrates the typical structure of the Schottky barrier [16] due to the electrical contact between the metal electrode (probe) and the semiconductor surface. CVC of the implanted material differs somewhat

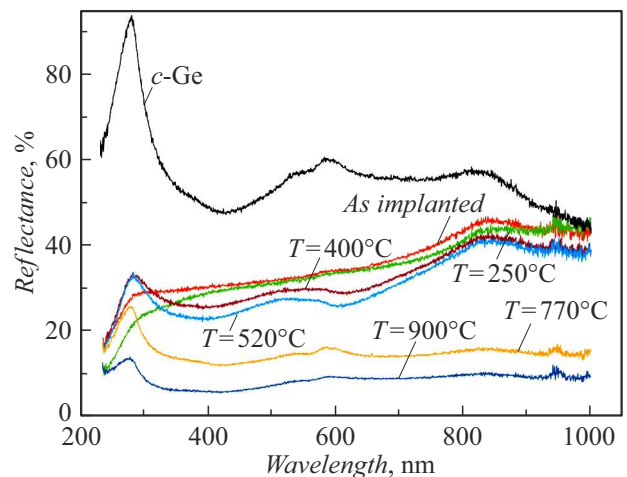


Figure 5. Optical reflectance spectra of *c*-Ge substrate and Ag:PGe samples before and after FTA.

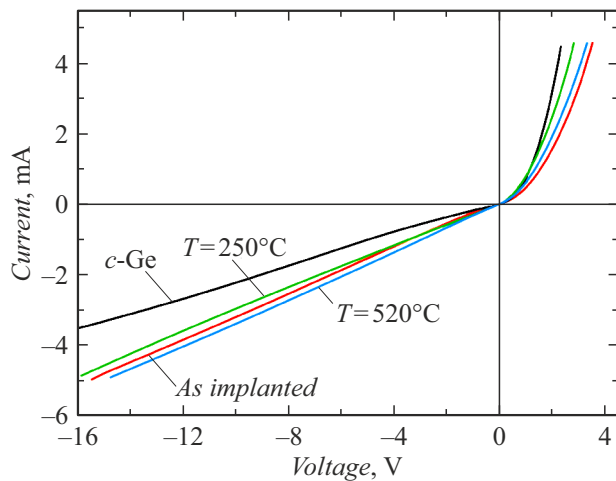


Figure 6. CVC for samples: *c*-Ge and samples Ag:PGe before and after FTA.

from the curve of the original substrate *c*-Ge. As can be seen from the positive branch, the voltage rises more slowly in the presence of the Ag:PGe layer on the substrate *c*-Ge compared to *c*-Ge, while the negative branch decreases more evidently in the implanted sample. A similar CVC behavior of a classical *c*-Ge photodiode and PGe layer formed by electrochemical anodization was observed in the paper [17]. It is obvious that CVC behavior for Ag:PGe is also determined by the Schottky barrier. Apparently, the difference between CVCs for *c*-Ge and Ag:PGe is due to the formation of the Ag:PGe layer on the *c*-Ge and the appearance of porous structure. In this case, the curve for the Ag:PGe sample is determined by the superposition of the conductivities in the implanted layer Ag:PGe and in the *c*-Ge substrate. FTA execution ($\tau = 1$ s $T = 250^\circ\text{C}$) leads to the fact that the positive branch of the CVC becomes steeper than that of the curve for the implanted sample Ag:PGe. It can be concluded that, as a result of FTA, the concentration of electric carriers in the near-surface layer becomes higher than in the substrate. This may be due to decrease in radiation defects as result of their annealing. The curve of the CVC negative branch of the annealed sample decreases somewhat more slowly than in the implanted material before annealing. After FTA ($\tau = 5$ s, $T = 520^\circ\text{C}$), the CVC becomes close to the dependence observed for Ag:PGe, which may be due to partial crystallization of the PGe layer after the annealing operation.

Conclusion

The paper discusses an experimental study of *c*-Ge substrates implanted with Ag^+ ions and subjected to FTA. It was shown that, as a result of ion implantation the amorphous porous Ag:PGe layer of spongy structure with nanowires is formed on the *c*-Ge surface. Annealing with τ increasing from 1 to 5 s leads to increase in the diameters of

the Ge nanowires making the sponge-like Ag:PGe structure from 26 to 35 nm. Annealing with τ greater than 5 s leads to destruction of the Ag:PGe porous structure and Ag evaporation from the samples. After FTA with $\tau = 3$ –9.5 s partial recrystallization of amorphous implanted Ag:PGe occurs.

Funding

The experiments on ion implantation and optical reflection were supported by the Russian Science Foundation grant № 19-79-10216, <https://rscf.ru/project/19-79-10216/>. Studies of pulsed light annealing and determination of current-voltage curves were carried out with the financial support of the Ministry of Science and Education of the Russian Federation as part of the State Assignment for the Federal Research Center „Kazan Scientific Center of the Russian Academy of Sciences“.

Conflict of interest

The authors declare that they have no conflict of interest.

References

- [1] S. Prucnal, L. Rebohle, W. Skorupa. *Mater. Sci. Semicond. Process.*, **62**, 115 (2017). DOI: 10.1016/j.mssp.2016.10.040
- [2] S. Prucnal, J. Zuk, R. Hübner, J. Duan, M. Wang, K. Pysznik, A. Drozdziel, M. Turek, S. Zhou. *Materials*, **13**, 1408 (2020). DOI: 10.3390/ma13061408
- [3] T.P. Gavrilova, S.M. Khantimerov, V.I. Nuzhdin, V.F. Valeev, A.M. Rogov, A.L. Stepanov. *Pis'ma v ZhTF* **48**, 33 (2022). (in Russian). DOI: 10.21883/PJTF.2022.08.52364.19096
- [4] A.L. Stepanov, V.I. Nuzhdin, A.M. Rogov, V.V. Vorob'ev. *Formirovanie cloev poristogo kremniya i germaniya s metallichesкими nanochastitsami* (Izd-vo FITS KazNTs RAN, Kazan, 2019) (in Russian)
- [5] P.W. Voorhees. *J. Stat. Phys.*, **38**, 231 (1985). DOI: 10.1007/BF01017860
- [6] A.F. Lopeandía, J. Rodríguez-Viejo. *Thermochim. Acta*, **461**, 82 (2007). DOI: 10.1016/j.tca.2007.04.010
- [7] H. Liu, S. Li, P. Sun, X. Yang, D. Liu, Y. Ji, F. Zhang, D. Chen, Y. Cui. *Mater. Sci. Semicond. Process.*, **83**, 58 (2018). DOI: 10.1016/j.mssp.2018.04.019
- [8] T.M. Donovan, W.E. Spicer, J.M. Bennett, E.J. Ashley. *Phys. Rev. B*, **2**, 397 (1970). DOI: 10.1103/PhysRevB.2.397
- [9] A.L. Stepanov, A.M. Rogov. *Opt. Commun.*, **474**, 126052 (2020). DOI: 10.1016/j.optcom.2020.126052
- [10] K.L. Bhatia, P. Singh, M. Singh, N. Kishore, N.C. Mehra, D. Kanjilal. *Nucl. Instrum. Methods Phys. Res. B*, **94**, 379 (1994). DOI: 10.1016/0168-583X(94)95412-7
- [11] Q.-C. Zhang, J.C. Kelly, M.J. Kenny. *Nucl. Instrum. Methods Phys. Res. B*, **47**, 257 (1990). DOI: 10.1016/0168-583X(90)90755-J
- [12] S. Schicho, A. Jaouad, C. Sellmer, D. Morris, V. Aimez, R. Arès. *Mater. Lett.*, **94**, 86 (2013). DOI: 10.1016/j.matlet.2012.12.014
- [13] A.V. Pavlikov, A.M. Rogov, A.M. Sharafutdinova, A.L. Stepanov. *Vacuum*, **184**, 109881 (2021). DOI: 10.1016/j.vacuum.2020.109881

- [14] S.A. Gavrilov, A.A. Dronov, I.M. Gavrilin, R.L. Volkov, N.I. Borgardt, A.Y. Trifonov, A.V. Pavlikov, P.A. Forsh, P.K. Kashkarov. *J. Raman Spectrosc.*, **49**, 810 (2018). DOI: 10.1002/jrs.5353
- [15] K. Boren, D. Huffman. *Pogloscheniye i rasseyaniye sveta malymi chastitsami* (Mir, M., 1986) (in Russian).
- [16] A. Dimoulas, P. Tsipas, A. Sotiropoulos. *Appl. Phys. Lett.*, **89**, 252110 (2006). DOI: 10.1063/1.2410241
- [17] E. Akkari, O. Touayar. *Int. J. Nanotechnology*, **10**, 553 (2013). DOI: 10.1504/IJNT.2013.053524